structure as determined via X-ray crystallography has no symmetry. The ^1H NMR spectra of the ring methylenes of both **2** and **3** appear as two A_4X doublets (J_{HP}). The chemical shift difference between these doublets is dictated by the substituents coordinated to the Au centers. A comparison of the ^1H NMR spectra of symmetrically substituted dihalogold(II) adducts[11,14] of **1** allows for a tentative assignment of the spectra. The downfield doublet is assigned to the methylenes proximal to the halide coordinated to the Au(II) center, and the upfield A_4X doublet arises from the methylenes nearest to the coordinated alkyl. The resonance of the methylenes in the alkyl moieties in **2** and **3** are further upfield (**2**, δ 2.16; **3** δ 2.30) than the methylene resonances in the noncoordinated alkyl iodides (CF_3CH_2I, δ 3.61 (q, J_{HF} = 9.9 Hz); CH_3CH_2I, δ 3.24 (q), 1.85 (t, J_{HH} = 7.4 Hz). In both complexes these methylenes appear as quartets with coupling to the three nearby spin $^1/_2$ nuclei.

Acknowledgment. These studies are supported by the National Science Foundation, Grant CHE 84-08414, and the donors of the Petroleum Research Fund, administered by the American Chemical Society. The Welch Foundation has supported some chemical purchases.

Registry No. **1**, 81457-56-9; **2**, 97374-16-8; **3**, 97374-17-9; CH_3CH_2I, 75-03-6; CF_3CH_2I, 353-83-3.

Supplementary Material Available: Tables of bond lengths and bond angels as well as anisotropic thermal parameters and structure factors (36 pages). Ordering information is given on any current masthead paper.

Hydroxy- and Hydrido-Bridged Binuclear Complexes of Iridium: Synthesis, Characterization, and Attempts To Model Binuclear Water-Gas Shift Catalysts. Structure of $[Ir_2(CO)_2(\mu\text{-}OH{\cdot}Cl)(Ph_2PCH_2PPh_2)_2]$

Bruce R. Sutherland and Martin Cowie*

Department of Chemistry, The University of Alberta, Edmonton, Alberta, Canada T6G 2G2

Received September 12, 1984

The reaction of *trans*-$[IrCl(CO)(DPM)]_2$ with excess NaOH yields $[Ir_2(CO)_2(\mu\text{-}OH{\cdot}Cl)(DPM)_2]$ which upon treatment with $HBF_4{\cdot}Et_2O$ gives $[Ir_2(CO)_2(\mu\text{-}OH)(DPM)_2][BF_4]$. Reaction of the former product with CO produces the binuclear Ir(0) complex $[Ir_2(CO)_4(DPM)_2]$ which after flushing with N_2 yields $[Ir_2(CO)_3(DPM)_2]$. Reaction of $[Ir_2(CO)_2(\mu\text{-}OH)(DPM)_2][BF_4]$ with CO produces $[Ir_2(CO)_2(\mu\text{-}H)(\mu\text{-}CO)(DPM)_2][BF_4]$. This latter complex reacts with $HBF_4{\cdot}Et_2O$ to give $[Ir_2(H)(CO)_2(\mu\text{-}H)(\mu\text{-}CO)(DPM)_2][BF_4]_2$ which rearranges with time yielding the isomeric complex $[Ir_2(H)_2(CO)_3(DPM)_2][BF_4]_2$. Reaction of either of these dihydrides with CO produces $[Ir_2(CO)_4(\mu\text{-}H)_2(DPM)_2][BF_4]_2$ and $[Ir_2(CO)_4(\mu\text{-}CO)(DPM)_2][BF_4]_2$ in the ratio 9:1, the latter product resulting from reductive elimination of H_2. Refluxing $[Ir_2(H)_2(CO)_3(DPM)_2][BF_4]_2$ in CH_3CN also produces some H_2 elimination and the formation of $[Ir_2(CO)_2(CH_3CN)_2(\mu\text{-}CO)(DPM)_2][BF_4]_2$. Reaction of $[Ir_2(CO)_4(\mu\text{-}CO)(DPM)_2][BF_4]_2$ with OH^- yields $[Ir_2(CO)_2(\mu\text{-}H)(\mu\text{-}CO)(DPM)_2][BF_4]$ whereas reaction of $[Ir_2(CO)_2(CH_3CN)_2(\mu\text{-}CO)(DPM)_2][BF_4]_2$ with OH^- gives a mixture of this hydride and the bridging hydroxide complex $[Ir_2(CO)_2(\mu\text{-}OH)(DPM)_2][BF_4]$. This chemistry is discussed and related to a model water-gas shift cycle. The related rhodium complex $[Rh_2(CO)_2(\mu\text{-}OH)(DPM)_2]^+$ is shown to be a WGS catalyst precursor under mild conditions, although it seems that metal hydrides and not hydroxides are the catalytically important species. The complex $[Ir_2(CO)_2(\mu\text{-}OH{\cdot}Cl)(DPM)_2]$ crystallizes in the space group $P2_12_12_1$ with a = 14.762 (2) Å, b = 25.583 (4) Å, c = 13.770 (3) Å, and Z = 4 and was refined to R = 0.043 and R_w = 0.065 based on 2650 unique observed reflections and 223 variables.

Introduction

The water-gas shift (WGS) reaction, shown in eq 1, is an industrially important process for increasing the H_2/CO ratio of synthesis gas.[1,2] At the present time this reaction

$$CO + H_2O \rightleftarrows CO_2 + H_2 \qquad (1)$$

utilizes heterogeneous catalysts (usually metal oxides) at high temperatures.[1] However, there has been increasing interest of late in the use of homogeneous catalysts which are active at lower temperatures[3-15] where the above equilibrium is more favorable.[16,17] One such study by Yoshida and co-workers, utilizing mononuclear rhodium

---

(1) "Catalyst Handbook"; Springer-Verlag: West Berlin, 1970; Chapters 5 and 6.

(2) Storch, H.; Golumbic, N.; Anderson, R. B. "The Fischer-Tropsch and Related Syntheses"; Wiley: New York, 1951.

(3) Laine, R. M.; Rinker, R. G.; Ford, P. C. *J. Am. Chem. Soc.* **1977**, *99*, 252.

(4) Kang, H. C.; Maudlin, C.; Cole, T.; Slegeir, W.; Cann, K.; Pettit, R. *J. Am. Chem. Soc.* **1977**, *99*, 8323.

(5) Cheng, C.-H., Hendriksen, D. E.; Eisenberg, R. *J. Am. Chem. Soc.* **1977**, *99*, 2791.

(6) King, R. B.; Fraier, C. C.; Hanes, R. M.; King, A. D. *J. Am. Chem. Soc.* **1978**, *100*, 2925.

(7) Ungermann, C.; Landis, V.; Moya, S. A.; Cohen, H.; Walker, H.; Pearson, R. G.; Rinker, R. G.; Ford, P. C. *J. Am. Chem. Soc.* **1979**, *101*, 5922.

(8) Ryan, R. C.; Wileman, G. M.; Dalsanto, M. P.; Pittman, C. U. *J. Mol. Catal.* **1979**, *5*, 319.

(9) King, A. D.; King, R. B.; Yang, D. B. *J. Am. Chem. Soc.* **1980**, *102*, 1028.

(10) Baker, E. C.; Hendrickson, D. E.; Eisenberg, R. *J. Am. Chem. Soc.* **1980**, *102*, 1020.

(11) Cheng, C.-H.; Eisenberg, R. *J. Am. Chem. Soc.* **1978**, *100*, 5968.

(12) Yoshida, T.; Ueda, Y.; Otsuka, S. *J. Am. Chem. Soc.* **1978**, *100*, 3941.

(13) (a) Kubiak, C. P.; Eisenberg, R. *J. Am. Chem. Soc.* **1980**, *102*, 3637. (b) Kubiak, C. P.; Woodcock, C.; Eisenberg, R. *Inorg. Chem.* **1982**, *21*, 2119.

0276-7333/85/2304-1637$01.50/0

Table I. Infrared Spectral Data (cm^{-1}) for the Compounds[a,b]

compound	solid[c]	solution[d]
$[Ir_2(CO)_2(\mu\text{-}OH{\cdot}Cl)(DPM)_2]$ (1)	1904 (m), 1882 (vs)	1889 (vs, br)
$[Ir_2(CO)_2(\mu\text{-}OH)(DPM)_2][BF_4]$ (2)	1959 (vs), 1943 (vs), 3498 (w)[e]	1956 (vs), 1935 (vs)
$[Ir_2(CO)_4(DPM)_2]$ (3)	1991 (s), 1982 (vs), 1974 (vs), 1922 (s), 1886 (s)	1990 (vs), 1977 (vs, br), 1928 (vs), 1895 (s, br)
$[Ir_2(CO)_3(DPM)_2]$ (4)	1950 (s), 1936 (vs), 1857 (s)	1996 (m), 1955 (vs), 1929 (vs), 1878 (s)
$[Ir_2(CO)_2(\mu\text{-}H)(\mu\text{-}CO)(DPM)_2][BF_4]$ (5)	1979 (m), 1967 (vs), 1826 (vs) (red) 1979 (m), 1967 (vs), 1850 (s) (orange)	1971 (vs, br), 1849 (s)
$[Ir_2(H)(CO)_2(\mu\text{-}H)(\mu\text{-}CO)(DPM)_2][BF_4]_2$ (6)	2046 (vs), 1961 (m), 1833 (m), 2108 (m)[f]	2060 (vs), 1969 (w), 1837 (s), 2115 (s)[f]
$[Ir_2(H)_2(CO)_3(DPM)_2][BF_4]_2$ (7)	2068 (m), 2031 (vs), 2136 (w),[f] 1957 (w)[f]	2070 (s), 2034 (vs)
$[Ir_2(CO)_4(\mu\text{-}H)_2(DPM)_2][BF_4]_2$ (8)	2080 (s), 2061 (m), 2038 (m), 2017 (w)	2085 (s), 2060 (m)
$[Ir_2(CO)_4(\mu\text{-}CO)(DPM)_2][BF_4]_2$ (9)	2091 (s), 2069 (vs), 2019 (s), 2026 (vs), 1792 (s)	*h*
$[Ir_2(CO)_2(CH_3CN)_2(\mu\text{-}CO)(DPM)_2][BF_4]_2$ (10)	2005 (s), 1980 (vs), 1731 (s), 2284 (w),[g] 2312 (w)[g]	*h*

[a] Abbreviations: vs = very strong, s = strong, m = medium, w = weak, br = broad. [b] All frequencies are carbonyl stretches unless otherwise noted. [c] Nujol mull. [d] CH_2Cl_2 solution. [e] ν(OH). [f] ν(IrH). [g] ν(CN). [h] Insoluble.

phosphine complexes,[14] rather elegantly demonstrated the involvement of both metal hydrides and metal hydroxides in the catalytic cycle.

We have recently been interested in small molecule activation and catalysis by binuclear complexes,[18-20] and part of this interest has been directed toward WGS chemistry. Of particular interest were binuclear carbonyl hydride and hydroxide complexes, analogous to the above-mentioned mononuclear species, in which the only ligands present, other than the phosphines, were those which could be actively involved in the WGS reaction. Two studies have already appeared in which the binuclear hydrides $[Rh_2(CO)_2(\mu\text{-}H)(\mu\text{-}CO)(DPM)_2]^+$[13] and $[Pt_2H_2(\mu\text{-}H)(DPM)_2]^+$[15] (DPM = $Ph_2PCH_2PPh_2$) were shown to be WGS catalysts or catalyst precursors. In neither of these systems was the involvement of metal hydroxides observed or inferred. We therefore undertook a study to investigate the possible involvement of binuclear hydroxides as catalysts. One such complex, $[Rh_2(CO)_2(\mu\text{-}OH)(DPM)_2][ClO_4]$, had been reported;[21] however, its catalytic activity had not been studied. Furthermore, this species was found, by ourselves and others,[21b] to be unreactive toward CO under ambient conditions. We therefore turned to the analogous chemistry of iridium anticipating that this system would be more reactive and might allow us to model WGS chemistry catalyzed by binuclear hydroxide complexes of rhodium and iridium. Herein, we report the results of this study.

Experimental Section

All solvents were appropriately dried and distilled prior to use and were stored under nitrogen. Reactions were performed under standard Schlenk conditions (using nitrogen which had previously been purified of remaining traces of oxygen and water using columns containing Ridox and 4A molecular sieves, respectively). Hydrated iridium(III) chloride was obtained from Johnson-Matthey, and bis(diphenylphosphino)methane (DPM) was purchased from Strem Chemicals. Carbon monoxide was obtained from Matheson and used as received. $[IrCl(C_8H_{14})_2]_2$,[22] $[Ir_2Cl(CO)_3(\mu\text{-}CO)(DPM)_2][Cl]$,[23] and $[IrCl(CO)(DPM)]_2$[23] were prepared by the reported procedures. Variable-temperature $^{31}P\{^1H\}$ NMR spectra were run on either a Bruker HFX-90 spectrometer operating at 36.43 MHz or a Bruker WH-400 spectrometer at 161.92 MHz; the temperature was measured with a thermocouple inserted directly into the probe. The spectra were recorded by using a external acetone-d_6 lock, and chemical shifts are referenced to 85% H_3PO_4. The ^1H NMR spectra were recorded on a Bruker WH-400 instrument. Infrared spectra were run on a Nicolet 7199 Fourier transform infrared spectrometer either as solids in Nujol mulls on KBr plates or as solutions in NaCl cells with 0.5-mm path length windows. Analyses were performed by the microanalytical service within the department.

The catalytic runs, using $[Rh_2(CO)_2(\mu\text{-}OH)(DPM)_2][BF_4]$ and $[Rh_2(CO)_2(\mu\text{-}H)(\mu\text{-}CO)(DPM)_2][BF_4]$ as catalyst precursors, were typically done by using 75 mg of compound in a mixture of 20 mL of 2-propanol and 2 mL of H_2O in a 100-mL flask. The vessel was charged with 1 atm of CO and heated to 80 °C. The gases, which were dried by passing them through a column of P_2O_5, were sampled into evacuated vessels and analyzed by mass spectrometry; the quantity of CO_2 was calculated on the basis of a comparison with a known amount of Ar added to the reaction vessel at the beginning of the reaction and the relative sensitivities of Ar and CO_2 taken from a 50:50 mixture of the two gases. A blank done under identical conditions, except that no catalyst was added, showed no CO_2.

Preparation of Compounds. (a) $[Ir_2(CO)_2(\mu\text{-}OH{\cdot}Cl)(DPM)_2]$ (1). To a slurry of 200 mg (0.156 mmol) of $[IrCl(CO)(DPM)]_2$ in THF was added 1.0 mL of a solution of ca. 2 M aqueous NaOH. Over a period of $^1/_2$ h, the solution color changed from purple to dark orange accompanied by the appearance of a bright orange solid. The solution was then taken to dryness in vacuo. To the resulting orange residue was added 10 mL of degassed H_2O and 20 mL of CH_2Cl_2, and the resulting mixture was stirred for 30 min. The two layers were allowed to separate, and the orange CH_2Cl_2 layer was removed and filtered under nitrogen. The volume of the filtrate was reduced to ca. 10 mL under an N_2 flow, and then 30 mL of Et_2O was added. This resulted in the precipitation of a finely divided light orange powder (150 mg, 76% yield). Compound 1 was determined to be a nonelectrolyte in CH_2Cl_2 solutions ($\Lambda(10^{-3}\ M) \leq 0.5\ \Omega^{-1}\ cm^2\ mol^{-1}$).[24,25] Spectroscopic parameters for this and all subsequent products are given in Tables I and II. Anal. Calcd for $Ir_2ClP_4O_3C_{52}H_{45}$: C, 49.50; H, 3.59; Cl, 2.81. Found: C, 49.73; H, 3.61; Cl, 2.76.

(b) $[Ir_2(CO)_2(\mu\text{-}OH)(DPM)_2][BF_4]$ (2). To a solution of 100 mg (0.079 mmol) of 1 in 10 mL of CH_2Cl_2 was added 1 equiv (11.4 μL) of $HBF_4{\cdot}Et_2O$ which produced an immediate darkening of the original orange solution. The addition of 30 mL of Et_2O resulted in the precipitation of an orange microcrystalline solid (95 mg, 92% yield). Conductivity measurements on a CH_2Cl_2 solution of this solid indicated that it was a 1:1 electrolyte ($\Lambda(10^{-3}$

---

(14) Yoshida, T.; Okana, T.; Ueda, Y.; Otsuka, S. *J. Am. Chem. Soc.* **1981**, *103*, 3411.

(15) Fisher, J. R.; Mills, A. J.; Sumner, S.; Brown, M. P.; Thomson, M. A.; Puddephatt, R. J.; Frew, A. A.; Manojlović-Muir, Lj.; Muir, K. W. *Organometallics* **1982**, *1*, 1421.

(16) Kassel, L. S. *J. Am. Chem. Soc.* **1934**, *56*, 1838.

(17) *K* for eq 1 = 1.45 × 10^3 at 127 °C and 26.9 at 327 °C, from ref 16.

(18) Cowie, M.; Dwight, S. K. *J. Organomet. Chem.* **1981**, *214*, 233.

(19) Cowie, M.; Southern, T. G. *Inorg. Chem.* **1982**, *21*, 246.

(20) Gibson, J. A. E.; Cowie, M. *Organometallics* **1984**, *3*, 984.

(21) (a) Deraniyagala, S. P.; Grundy, K. R. *Inorg. Chem.* **1985**, *24*, 50. (b) Deraniyagala, S. P. Ph.D. Thesis, Dalhousie University, 1984.

(22) Herde, J. L.; Lambert, J. C.; Senoff, C. V. *Inorg. Synth.* **1974**, *15*, 18.

(23) Cowie, M.; Sutherland, B. R. *Inorg. Chem.* **1984**, *23*, 2324.

(24) A typical 1:1 electrolyte of this type $[Rh_2(CO)_2(\mu\text{-}Cl)(\mu\text{-}CO)(DPM)_2][BPh_4]$, for example, gives $\Lambda(10^{-3}\ M) = 45.8\ \Omega^{-1}\ cm^2\ mol^{-1}$ in CH_2Cl_2.

(25) For typical conductivities in various solvents see: Geary, W. J. *Coord. Chem. Rev.* **1971**, *7*, 81.

Table II. NMR Spectral Data for the Compounds[a]

compound	$^{31}P\{^1H\}$,[b] ppm	^1H,[c] ppm
$[Ir_2(CO)_2(\mu\text{-}OH{\cdot}Cl)(DPM)_2]$ (1)	11.1 (s)	7.74–7.13 (m, 40 H), 4.85 (q, 1 H, $^2J_{P-H} \simeq 3.5$ Hz), 5.4 (vbr, 2 H) 2.8 (vbr, 2 H)
$[Ir_2(CO)_2(\mu\text{-}OH)(DPM)_2][BF_4]$ (2)	13.7 (s)	7.77–7.21 (m, 40 H), 4.19 (m, 2 H), 3.32 (m, 2 H), 2.03 (q, 1 H, $^2J_{P-H} = 3.1$ Hz)
$[Ir_2(CO)_4(DPM)_2]$ (3)	−22.8 (s)	7.30–7.06 (m, 40 H), 4.83 (vbr, 4 H)
$[Ir_2(CO)_3(DPM)_2]$ (4)	−3.6 (s)	7.46–7.20 (m, 40 H), 4.92 (s, 4 H)
$[Ir_2(CO)_2(\mu\text{-}H)(\mu\text{-}CO)(DPM)_2][BF_4]$ (5)	+9.1 (s)	7.49–7.30 (m, 40 H), 3.87 (s, br, 4 H), −9.44 (q, 1 H, $^2J_{P-H} = 9.4$ Hz)
$[Ir_2(H)(CO)_2(\mu\text{-}H)(\mu\text{-}CO)(DPM)_2][BF_4]_2$ (6)	14.4 (m), −2.9 (m)	7.71–7.25 (m, 40 H), 4.59 (m, br, 4 H), −7.11 (m, br 1 H), −13.19 (td, 1 H, $^2J_{P-H} = 10.5$ Hz, $^2J_{H-H} = 1.6$ Hz)
$[Ir_2(H)_2(CO)_3(DPM)_2[BF_4]_2$ (7)	−12.3 (m), −17.7 (m)	7.56–7.32 (m, 40 H), 5.68 (m, 2 H), 4.90 (m, 2 H) −9.83 (t, 1 H, $^2J_{P-H} = 7.9$ Hz), −17.42 (t, 1 H, $^2J_{P-H} = 11.2$ Hz)
$[Ir_2(CO)_4(\mu\text{-}H)_2(DPM)_2][BF_4]_2$ (8)	−18.8 (s)	7.53–7.47 (m, 40 H), 5.34 (vbr, 4 H), −9.66 (q, 2 H, $^2J_{P-H} = 5.1$ Hz)
$[Ir_2(CO)_4(\mu\text{-}CO)(DPM)_2][BF_4]_2$ (9)	−15.3 (s)	7.77–7.45 (m, 40 H), 5.84 (q, 4 H, $^2J_{P-H} = 4.8$ Hz)
$[Ir_2(CO)_2(CH_3CN)_2(\mu\text{-}CO)(DPM)_2][BF_4]_2$ (10)	−7.5 (s)	7.67–7.22 (m, 40 H), 4.19 (m, 2 H), 3.35 (m, 2 H), 1.27 (s, 6 H)[d]

[a] Abbreviations used: s = singlet, t = triplet, td = triplet of doublets, q = quintet, m = multiplet, br = broad, vbr = very broad. [b] vs. 85% H_3PO_4, −40 °C. [c] In CD_2Cl_2 at +25 °C. [d] In acetone-d_6.

M) = 41.8 Ω^{-1} cm^2 mol^{-1}). Anal. Calcd for $Ir_2P_4F_4O_3C_{52}BH_{45}$: C, 47.56; H, 3.45; Cl, 0.0. Found: C, 47.57; H, 3.87; Cl, 0.0.

(c) $[Ir_2(CO)_4(DPM)_2]{\cdot}CH_2Cl_2$[26] (3). A CH_2Cl_2 solution of 1 (100 mg, 0.079 mmol, in 10 mL) was stirred under an atmosphere of CO for 30 min during which time the color changed from orange to bright yellow. Et_2O (30 mL), saturated with carbon monoxide, was added to the solution which was then stored at −15 °C overnight. During this time bright yellow crystals of 3 appeared. This solid was determined to be very susceptible to CO loss and was stored in a sealed flask under a CO atmosphere. The yield was 95 mg (90%). Solutions of 3 in CH_2Cl_2 were nonconducting ($\Lambda(10^{-3}$ M) ≤ 0.5 Ω^{-1} cm^2 mol^{-1}). Anal. Calcd for $Ir_2Cl_2P_4O_4C_{55}H_{46}$: C, 48.93; H, 3.43. Found: C, 49.01; H, 3.39.

(d) $[Ir_2(CO)_3(DPM)_2]$ (4). Dinitrogen was bubbled through a CH_2Cl_2 solution of 3 (100 mg, 0.079 mmol, in 10 mL) for 10 min during which time the solution changed color from bright yellow to dark golden yellow. The solution was taken to dryness under an N_2 stream leaving a dark yellow-brown residue. Recrystallization of this solid from THF/Et_2O produced a golden yellow finely divided powder (85 mg, 87% yield). Compound 4 was determined to be a nonelectrolyte in CH_2Cl_2 solutions ($\Lambda(10^{-3}$ M) ≤ 0.5 Ω^{-1} cm^2 mol^{-1}). Anal. Calcd for $Ir_2P_4O_3C_{53}H_{44}$: C, 51.45; H, 3.58; Cl, 0.00. Found: C, 51.42; H, 3.80; Cl, 0.05.

(e) $[Ir_2(CO)_2(\mu\text{-}H)(\mu\text{-}CO)(DPM)_2][BF_4]$ (5). Method A. A solution of $[Ir_2(CO)_2(\mu\text{-}OH)(DPM)_2][BF_4]$ in CH_2Cl_2 (100 mg, 0.076 mmol, in 10 mL) was stirred under an atmosphere of carbon monoxide for 30 min during which time the solution changed color from red-orange to yellow-orange. The solution was taken to dryness under an N_2 stream leaving a dark red residue. Recrystallization from CH_2Cl_2/Et_2O gave either a red orange or a dark red-purple crystalline solid (90 mg, 89% yield) (see Discussion). A CH_2Cl_2 solution of this solid indicated that 5 was 1:1 electrolyte ($\Lambda(10^{-3}$ M) = 45.7 Ω^{-1} cm^2 mol^{-1}). Anal. Calcd for $Ir_2P_4F_4O_3C_{53}BH_{45}$: C, 48.04; H, 3.42. Found: C, 47.72; H, 3.59.

Method B. To a solution of $[Ir_2(CO)_3(DPM)_2]$ (4) in CH_2Cl_2 (100 mg in 10 mL) was added 1 equiv (11.6 μL) of $HBF_4{\cdot}Et_2O$. The solution immediately changed color from golden yellow to dark red. Et_2O (30 mL) was added and resulted in the precipitation of a dark red crystalline material which was in all of its spectroscopic properties identical with that isolated from method A.

(f) $[Ir_2(H)(CO)_2(\mu\text{-}H)(\mu\text{-}CO)(DPM)_2][BF_4]_2$ (6). To a solution of $[Ir_2(CO)_2(\mu\text{-}H)(\mu\text{-}CO)(DPM)_2][BF_4]$ in CH_2Cl_2 (100 mg, 0.075 mmol, in 10 mL) was added 1 equiv of $HBF_4{\cdot}Et_2O$ (10.8 μL) whereupon the solution immediately changed color from dark red to bright yellow. The solution volume was reduced to ca. 5 mL under an N_2 stream. The addition of 15 mL of hexanes caused the precipitation of a golden yellow, extremely moisture-sensitive solid (85 mg, 80% yield). Conductivity measurements in CH_2Cl_2 gave values which were low ($\Lambda(10^{-3}$ M) = 41.9 Ω^{-1} cm^2 mol^{-1}); however in nitromethane this species behaved as a normal 2:1 electrolyte ($\Lambda(10^{-3}$ M) = 219.2 Ω^{-1} cm^2 mol^{-1}). Anal. Calcd for $Ir_2P_4F_8O_3C_{53}B_2H_{46}$: C, 45.06; H, 3.28. Found: C, 45.05; H, 3.23.

(g) $[Ir_2(CO)_4(\mu\text{-}H)_2(DPM)_2][BF_4]_2$ (8). A solution of 6 (100 mg, 0.070 mmol, in 10 mL of CH_2Cl_2) was stirred under an atmosphere of carbon monoxide. Within 5 min the solution color had changed from yellow to almost colorless pale yellow. The addition of 30 mL of Et_2O resulted in the precipitation of a white solid. This solid was redissolved in 5 mL of CH_2Cl_2 and filtered under carbon monoxide. Hexanes (10 mL) was added to the filtrate, and the solution was stored under a CO atmosphere at −15 °C overnight during which time 8 precipitated as a white microcrystalline solid (90 mg, 89% yield). The conductivity in CH_2Cl_2 solution was $\Lambda(10^{-3}$ M) = 37.3 Ω^{-1} cm^2 mol^{-1} whereas in nitromethane $\Lambda(10^{-3}$ M) = 178.8 Ω^{-1} cm^2 mol^{-1}. Anal. Calcd for $Ir_2P_4F_8O_4C_{54}B_2H_{46}$: C, 45.01; H, 3.22. Found: C, 42.58; H, 3.30.[27]

(h) $[Ir_2(CO)_4(\mu\text{-}CO)(DPM)_2][BF_4]_2{\cdot}(CH_3)_2CO$ (9).[26] To a solution of $[Ir_2Cl(CO)_3(\mu\text{-}CO)(DPM)_2][Cl]$ in CH_2Cl_2 under CO (297 mg, 0.222 mmol, in 10 mL) was added dropwise a solution of 2 equiv of $AgBF_4$ (86.7 mg) dissolved in 5 mL of THF. No change was observed until more than half of the solution had been added after which point the solution darkened rapidly and a light yellow precipitate appeared. The solution was stirred under CO for 30 min, and then 30 mL of Et_2O was added to induce complete precipitation. The supernatant was removed, and the solid was dried under a CO stream. The residue was redissolved in 15 mL of acetone and filtered under a CO atmosphere, giving a pale yellow solution. The addition of 50 mL of Et_2O resulted in the precipitation of a white microcrystalline solid (250 mg, 78% yield). Conductivity measurements in acetone indicated that 9 was a 2:1 electrolyte[25] ($\Lambda(10^{-3}$ M) = 238.6 Ω^{-1} cm^2 mol^{-1}). Anal. Calcd for $Ir_2P_4F_8O_6C_{58}B_2H_{50}$: C, 45.68; H, 3.31. Found: C, 45.46; H, 3.49.

(i) $[Ir_2(CO)_2(CH_3CN)_2(\mu\text{-}CO)(DPM)_2][BF_4]_2$ (10). A slurry of 9 was prepared by adding 10 mL of CH_2Cl_2 to 250 mg (0.174 mmol) of the solid. Dry CH_3CN (2 mL) was then added resulting in immediate gas evolution and the formation of a clear pale yellow solution. The system was then purged with N_2 for 15 min during which time a white microcrystalline solid began to form. Stirring was discontinued after 2 h, and the reaction flask was then placed in the freezer at −15 °C overnight during which time a large amount of white precipitate appeared. Complete precipitation was induced by the addition of 30 mL of Et_2O. This solid was collected and washed twice with 10-mL portions of Et_2O and dried under an N_2 stream (210 mg, 82% yield). Conductivity measurements of 10 in CH_3CN showed it to be a 2:1 electrolyte ($\Lambda(10^{-3}$ M) = 229.4 Ω^{-1} cm^2 mol^{-1}). Anal. Calcd for $Ir_2P_4F_8O_3N_2C_{57}B_2H_{50}$: C, 45.86; H, 3.38; N, 1.88. Found: C, 45.02; H; 3.40; N, 1.80.

(j) $[Ir_2(H)_2(CO)_3(DPM)_2][BF_4]_2$ (7). An atmosphere of H_2 was placed over a slurry of 200 mg of 10 in 10 mL of CH_2Cl_2 and the resulting mixture stirred vigorously. After 20 min all of the solid had dissolved producing a clear light yellow solution. The excess hydrogen was then removed by purging the solution with N_2 for 15 min eventually producing a darker yellow solution. Hexanes (30 mL) was added and resulted in the precipitation of a white microcrystalline solid. The mother liquor was removed and the resulting solid dried initially under an N_2 stream and

---

[26] The presence of one molecule of crystallization was confirmed by ^1H NMR spectroscopy.

[27] Attempts to obtain a satisfactory analysis for 8 have been frustrated by its rapid decomposition.

finally in vacuo for 2 h. Typical isolated yields of this highly moisture-sensitive compound were 80–90%. Conductivity measurements on **7** in CH_2Cl_2 gave $\Lambda(10^{-3}\ M) = 40.7\ \Omega^{-1}\ cm^2\ mol^{-1}$ but in nitromethane gave $\Lambda(10^{-3}\ M) = 173.6\ \Omega^{-1}\ cm^2\ mol^{-1}$. Anal. Calcd for $Ir_2P_4F_8O_3C_{53}B_2H_{46}$: C, 45.06; H, 3.28. Found: C, 44.98; H, 3.31.

Reaction of 9 with $NMe_4OH{\cdot}5H_2O$. To a solution of **9** in acetone (265 mg in 10 mL) was added 1 equiv of $NMe_4OH{\cdot}5H_2O$ (32.7 mg) in 1 mL of degassed H_2O. The solution color immediately changed from pale yellow to bright yellow, and a bright yellow solid precipitated. The color then rapidly faded to dull yellow-orange, and the precipitate began to redissolve. Concentrating the solution under an N_2 stream caused it to turn bright red. The solution was taken to dryness in vacuo leaving a bright red residue. This solid was redissolved in CH_2Cl_2, filtered under N_2, and precipitated by the addition of Et_2O resulting in a bright red microcrystalline product. Spectroscopic examination showed this solid to be $[Ir_2(CO)_2(\mu\text{-}H)(\mu\text{-}CO)(DPM)_2][BF_4]$ (**5**).

Reaction of 10 with $NMe_4OH{\cdot}5H_2O$. To a solution of **10** in acetonitrile (55 mg in 5 mL) was added 1 equiv of $NMe_4OH{\cdot}5H_2O$ (6.5 mg) in 1 mL of degassed H_2O. The solution color immediately changed from yellow to orange. The solvent was removed in vacuo leaving a dark orange powder. This was then redissolved in CH_2Cl_2 and filtered under N_2. Addition of 30 mL of ether resulted in the precipitation of an orange solid which was shown by spectroscopic means to be a mixture of **2** and **5** (ratio ~3:1).

Reaction of 10 with NaO_2CH. To a solution of **10** in acetonitrile (150 mg in 5 mL) was added 1 equiv of NaO_2CH (6.8 mg) in 1 mL of acetonitrile. Over a period of 1 h the solution color changed from yellow to bright red and coincided with the appearance of a red solid. The solution was taken to dryness under vacuum and then redissolved in CH_2Cl_2 giving a bright red solution and filtered under N_2. Addition of 30 mL of ether resulted in the precipitation of a bright red solid which was shown by IR and NMR (^1H, ^{31}P) spectroscopy to be $[Ir_2(CO)_2(\mu\text{-}H)(\mu\text{-}CO)(DPM)_2][BF_4]$ (**5**).

Reaction of 10 with NaOMe. To a solution of **10** in acetonitrile (225 mg in 5 mL) was added 1 equiv of NaOMe (8.0 mg) in 1 mL of MeOH which had been freshly distilled from magnesium turnings. The solution immediately changed from yellow to bright red. This was taken to dryness in vacuo and then redissolved in CH_2Cl_2 giving a bright red solution which was filtered under N_2. Addition of 30 mL of ether resulted in the precipitation of a bright red solid which was shown by means of IR and NMR (^1H and ^{31}P) spectroscopy to be **5**.

X-ray Data Collection. An orange crystal of $[Ir_2(CO)_2(\mu\text{-}OH{\cdot}Cl)(DPM)_2]$, obtained by the slow diffusion of diethyl ether into a saturated CH_2Cl_2 solution of the complex, was mounted in a glass capillary under N_2. Preliminary film data showed that the crystal belonged to the orthorhombic system, with systematic absences ($h00$, h = odd; $0k0$, k = odd; $00l$, l = odd) consistent with the space group $P2_12_12_1$. Accurate cell parameters were obtained from a least-squares refinement of the setting angles of 23 reflections, in the range $15.0 \leq 2\theta \leq 28.2°$, which were accurately centered on an Enraf-Nonius CAD-4 diffractometer using Mo Kα radiation. See Table III for pertinent crystal and data collection details.

Intensity data were collected on a CAD-4 diffractometer in the bisecting mode and employing the ω-2θ scan technique up to $2\theta = 50.0°$ with graphite-monochromated Mo Kα radiation. Backgrounds were scanned for 25% of the peak width on either end of the peak scan. The intensities of three standard reflections were measured every 1 h of exposure to assess possible crystal decomposition. No significant decay of these standards was observed over the course of the data collection, so no correction was applied to the data. A total of 4781 unique reflections were measured and processed in the usual way using a value of 0.04 for p;[28] of these 2650 had $F_o^2 \geq 3\sigma(F_o^2)$ and were used in subsequent calculations. Absorption corrections were applied to the data by using Gaussian integration.[29]

Table III. Summary of Crystal Data and Details of Intensity Collection

compd	$[Ir_2(CO)_2(\mu\text{-}OH{\cdot}Cl)(DPM)_2]$
fw	1261.68
formula	$Ir_2ClP_4O_3C_{52}H_{45}$
space group	$P2_12_12_1$
Z	4
cell parameters	
a, Å	14.762 (2)
b, Å	25.583 (4)
c, Å	13.770 (3)
V, Å	5200.3
ρ(calcd), g/cm^3	1.611
temp, °C	22
radiatn	Mo Kα (λ = 0.71069 Å), graphite monochromated
receiving, aperture, mm	2.00 + 0.500 tan θ wide × 4.0 high, 173 from crystal
takeoff angle, deg	2.55
scan speed, deg/min	variable from 10.058 and 1.804
scan width, deg	0.75 + 0.350 tan θ in ω
2θ limits, deg	$3.0 \leq 2\theta \leq 50.0$
μ, cm^{-1}	53.041
range in abs corr factors (as applied to F_o^2)	0.406–0.504
cryst shape	orthorthombic prism with faces of the form {120}, {011}, and {021}
unique data collected	4781
unique data used ($F_o^2 \geq 3\sigma(R_o^2)$)	2650
final no. of parameters refined	223
error in observn of unit weight	1.516
R	0.043
R_w	0.065

Structure Solution and Refinement. The structure was solved in the space group $P2_12_12_1$ with the use of a Patterson map to locate the two independent Ir atoms. Subsequent refinements and differences Fourier syntheses led to location of all remaining non-hydrogen atoms. Atomic scattering factors were taken from Cromer and Waber's tabulation[30] for all atoms except hydrogen, for which the values of Stewart et al. were used.[31] Anomalous dispersion terms for Ir, Cl, and P were included in F_c.[32] All phenyl ring carbon atoms were refined as rigid groups having D_{6h} symmetry, C–C distances of 1.392 Å, and independent isotropic thermal parameters. All hydrogen atoms, except that of the bridging OH·Cl unit, were input as fixed contributions; their idealized positions were calculated after each cycle of refinement from the geometries of their attached carbon atoms using a C–H distance of 0.95 Å. These hydrogen atoms were assigned isotropic thermal parameters of 1 Å^2 greater than the B (or equivalent isotropic B) of their attached carbon atom.

A difference Fourier map phased on all of the non-hydrogen atoms and using a $(\sin\theta)/\lambda$ cutoff value of 0.35 Å^{-1} revealed the hydrogen atom of the bridging OH·Cl unit as the largest peak. Attempted refinement of this hydrogen (H(1)) resulted in slow divergence of its thermal parameter. In subsequent refinements this atom was given a fixed thermal parameter and position corresponding to its position in the Fourier map and was not refined. All other non-hydrogen atoms were refined anisotropically.

The final model with 223 parameters refined converged to $R = 0.043$ and $R_w = 0.065$.[33] On the final difference Fourier map the 20 highest peaks (1.75–0.54 e Å^{-3}) were in the vicinities of the phenyl groups and the Ir and P atoms. A typical carbon atom on earlier syntheses had a peak intensity of about 3.5 e Å^{-3}.

Refinement of the structure as the other enantiomer resulted in higher residuals ($R = 0.054$ and $R_w = 0.076$) and slightly larger

---

(28) Doedens, R. J.; Ibers, J. A. *Inorg. Chem.* **1967**, *6*, 204.

(29) For the programs used in the solution and refinement of the structure, see ref 23.

(30) Cromer, D. T.; Waber, J. T. "International Tables for Crystallography"; Kynoch Press: Birmingham, England, 1974; Vol. IV, Table 2.2A.

(31) Stewart, R. F.; Davidson, E. R.; Simpson, W. T. *J. Chem. Phys.* **1965**, *42*, 3175.

(32) Cromer, D. T.; Liberman, D. *J. Chem. Phys.* **1970**, *53*, 1891.

(33) $R = \sum||F_o| - |F_c||/\sum|F_o|$; $R_w = [\sum w(|F_o| - |F_c|)^2/\sum wF_o^2]^{1/2}$.

Table IV. Positional and Thermal Parameters for the Nongroup Atoms of $[Ir_2(CO)_2(\mu\text{-}OH \bullet Cl)(DPM)_2]$

atom	x[a]	y	z	B, Å^2	atom	x	y	z	B, Å^2
Ir(1)	0.06260 (9)	0.17389 (6)	0.26839 (10)	2.68[b]	O(2)	−0.090 (2)	0.016 (1)	0.019 (2)	6.7[b]
Ir(2)	−0.04077 (8)	0.12183 (5)	0.09339 (9)	2.68[b]	O(3)	−0.001 (1)	0.1946 (7)	0.140 (1)	3.3[b]
Cl(1)	−0.1366 (6)	0.2867 (4)	0.1301 (7)	4.8[b]	C(1)	0.119 (3)	0.163 (2)	0.379 (3)	5.8[b]
P(1)	−0.0725 (6)	0.1709 (4)	0.3532 (6)	3.1[b]	C(2)	−0.069 (2)	0.054 (2)	0.048 (3)	6.4[b]
P(2)	−0.1769 (6)	0.1300 (4)	0.1768 (6)	3.0[b]	C(3)	−0.173 (2)	0.176 (1)	0.273 (2)	3.6[b]
P(3)	0.1937 (6)	0.1796 (4)	0.1769 (6)	2.6[b]	C(4)	0.172 (2)	0.173 (1)	0.048 (2)	2.9[b]
P(4)	0.0980 (5)	0.1193 (4)	0.0130 (6)	2.8[b]	H(1)	−0.053	0.219	0.143	4.0
O(1)	0.157 (2)	0.159 (1)	0.456 (2)	7.9[b]					

[a] Estimated standard deviations in the last significant figure(s) are given in parentheses in this and all subsequent tables. [b] Equivalent isotropic B's for anisotropic atoms.

Table V. Derived Parametes for the Rigid Groups of $[Ir_2(CO)_2(\mu\text{-}OH \bullet Cl)(DPM)_2]$

atom	x	y	z	B, Å^2	atom	x	y	z	B, Å^2
C(11)	−0.0914 (16)	0.1128 (8)	0.4271 (15)	3.0 (7)	C(51)	0.2488 (16)	0.2442 (8)	0.1858 (19)	3.8 (8)
C(12)	−0.1710 (14)	0.1097 (8)	0.4810 (18)	4.9 (9)	C(52)	0.3100 (17)	0.2617 (9)	0.1162 (14)	5.3 (10)
C(13)	−0.1887 (14)	0.0656 (11)	0.5371 (16)	5.6 (10)	C(53)	0.3546 (15)	0.3091 (10)	0.1291 (17)	4.9 (9)
C(14)	−0.1268 (18)	0.0246 (8)	0.5392 (16)	4.6 (9)	C(54)	0.3381 (18)	0.3390 (8)	0.2116 (21)	6.0 (10)
C(15)	−0.0473 (16)	0.0276 (8)	0.4853 (18)	5.4 (9)	C(55)	0.2769 (20)	0.3215 (11)	0.2813 (16)	8.8 (13)
C(16)	−0.0296 (12)	0.0717 (10)	0.4292 (15)	5.0 (9)	C(56)	0.2323 (15)	0.2741 (11)	0.2684 (16)	5.5 (9)
C(21)	−0.0854 (17)	0.2230 (9)	0.4413 (19)	4.2 (8)	C(61)	0.2845 (14)	0.1323 (8)	0.2004 (17)	2.5 (7)
C(22)	−0.1237 (16)	0.2702 (12)	0.4122 (15)	6.4 (10)	C(62)	0.2696 (13)	0.0907 (10)	0.2636 (16)	5.4 (9)
C(23)	−0.1283 (17)	0.3119 (8)	0.4769 (24)	6.8 (11)	C(63)	0.3374 (18)	0.0538 (8)	0.2790 (16)	5.5 (9)
C(24)	−0.0947 (20)	0.3064 (11)	0.5708 (21)	8.0 (13)	C(64)	0.4200 (15)	0.0584 (9)	0.2311 (19)	5.6 (9)
C(25)	−0.0564 (19)	0.2593 (14)	0.5999 (15)	9.8 (14)	C(65)	0.4349 (13)	0.0999 (10)	0.1678 (18)	6.6 (10)
C(26)	−0.0517 (17)	0.2176 (9)	0.5351 (22)	8.3 (12)	C(66)	0.3672 (17)	0.1369 (8)	0.1525 (15)	5.9 (10)
C(31)	−0.2720 (13)	0.1512 (9)	0.1108 (17)	2.8 (7)	C(71)	0.0900 (15)	0.1232 (10)	−0.1203 (11)	3.6 (7)
C(32)	−0.2922 (17)	0.1233 (8)	0.0267 (19)	5.9 (10)	C(72)	0.0396 (14)	0.0849 (8)	−0.1675 (16)	4.0 (8)
C(33)	−0.3667 (19)	0.1374 (11)	−0.0295 (15)	11.3 (17)	C(73)	0.0329 (14)	0.0852 (8)	−0.2683 (16)	4.5 (8)
C(34)	−0.4209 (14)	0.1793 (11)	−0.0017 (17)	5.0 (9)	C(74)	0.0767 (18)	0.1237 (10)	−0.3220 (11)	5.6 (9)
C(35)	−0.4006 (16)	0.2071 (8)	0.0824 (19)	6.0 (10)	C(75)	0.1272 (16)	0.1620 (8)	−0.2748 (18)	6.1 (10)
C(36)	−0.3262 (17)	0.1931 (9)	0.1386 (14)	4.4 (9)	C(76)	0.1338 (14)	0.1618 (8)	−0.1740 (19)	5.5 (10)
C(41)	−0.2227 (15)	0.0710 (7)	0.2329 (15)	2.9 (6)	C(81)	0.1683 (17)	0.0599 (9)	0.0292 (21)	3.3 (8)
C(42)	−0.3110 (14)	0.0710 (8)	0.2682 (17)	4.5 (8)	C(82)	0.2424 (20)	0.0532 (11)	−0.0320 (17)	6.7 (11)
C(43)	−0.3459 (13)	0.0265 (11)	0.3128 (17)	6.5 (11)	C(83)	0.2957 (16)	0.0085 (14)	−0.0245 (22)	10.6 (17)
C(44)	−0.2924 (19)	−0.0180 (8)	0.3222 (17)	6.0 (10)	C(84)	0.2748 (21)	−0.0295 (10)	0.0443 (27)	8.3 (14)
C(45)	−0.2041 (18)	−0.0180 (7)	0.2869 (18)	6.5 (11)	C(85)	0.2007 (24)	−0.0228 (11)	0.1055 (21)	9.7 (15)
C(46)	−0.1692 (12)	0.0265 (9)	0.2423 (16)	3.7 (7)	C(86)	0.1475 (17)	0.0219 (13)	0.0979 (19)	9.0 (14)

Rigid-Group Parameters

	X_c	Y_c	Z_c	ϕ	θ	ρ
group 1	−0.1091 (11)	0.0687 (6)	0.4832 (10)	−2.006 (15)	2.841 (14)	0.620 (14)
group 2	−0.0900 (11)	0.2647 (8)	0.5060 (14)	−2.474 (23)	−2.363 (18)	2.022 (23)
group 3	−0.3464 (11)	0.1652 (7)	0.0546 (11)	0.274 (20)	−2.448 (16)	−2.33 (19)
group 4	−0.2576 (11)	0.0265 (6)	0.2776 (10)	−2.069 (15)	2.993 (15)	0.463 (14)
group 5	0.2935 (11)	0.2916 (7)	0.1987 (12)	1.302 (33)	−2.087 (15)	0.261 (32)
group 6	0.3523 (11)	0.0953 (6)	0.2157 (10)	−0.884 (20)	2.454 (15)	0.198 (18)
group 7	0.0834 (9)	0.1235 (6)	−0.2212 (11)	−0.616 (13)	3.105 (15)	−1.631 (15)
group 8	0.2216 (13)	0.0152 (8)	0.0367 (14)	2.090 (32)	−2.305 (17)	3.030 (29)

[a] X_c, Y_c, and Z_c are the fractional coordinates of the centroid of the rigid group. The rigid-group orientation angles ϕ, θ, and ρ have been defined before: La Placa, S. J.; Ibers, J. A. *Acta Crystallogr.* **1965**, *18*, 511.

thermal parameters for all atoms suggesting that the original choice was the correct one.

The final positional parameters of the individual non-hydrogen atoms and the phenyl groups are given in Tables IV and V, respectively. Tables of derived hydrogen parameters and anisotropic thermal parameters and a listing of observed and calculated structure amplitudes used in the refinements are available.[34]

Results and Discussion

(a) Description of Structure. As shown in Figure 1, $[Ir_2(CO)_2(\mu\text{-}OH{\cdot}Cl)(DPM)_2]$ displays an "A-frame" type structure in which the apical site is occupied by the bridging OH·Cl moiety with the two terminal carbonyl groups almost trans to the iridium–oxygen bonds. The bridging DPM ligands are coordinated in mutually trans positions, essentially perpendicular to the Ir–O–Ir plane, much as is observed in other DPM-bridged complexes. As

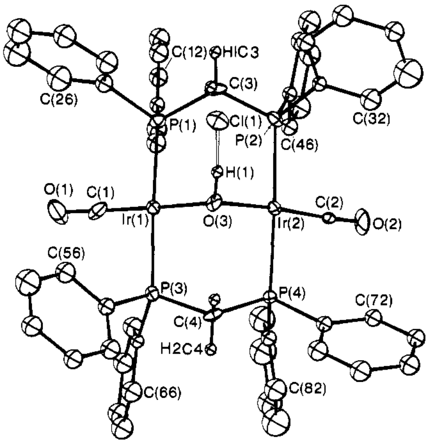

Figure 1. Perspective view of $[Ir_2(CO)_2(\mu\text{-}OH{\cdot}Cl)(DPM)_2]$, showing the numbering scheme. The numbering on the phenyl carbon atoms starts at the carbon atom bonded to phosphorus and increases sequentially around the ring. The 20% thermal ellipsoids are shown.

---

(34) Supplementary material.

Table VI. Selected Distances (Å) in $[Ir_2(CO)_2(\mu\text{-}OH\bullet Cl)(DPM)_2]$

	Bonding Distances		
Ir(1)-O(3)	2.07 (2)	P(1)-C(3)	1.85 (3)
Ir(2)-O(3)	2.06 (2)	P(2)-C(3)	1.78 (4)
Ir(1)-C(1)	1.75 (5)	P(3)-C(4)	1.81 (3)
Ir(2)-C(2)	1.89 (4)	P(4)-C(4)	1.82 (4)
Ir(1)-P(1)	2.312 (9)	P(1)-C(11)	1.82 (2)
Ir(1)-P(3)	2.313 (9)	P(1)-C(21)	1.81 (3)
Ir(2)-P(2)	2.323 (9)	P(2)-C(31)	1.76 (2)
Ir(2)-P(4)	2.330 (8)	P(2)-C(41)	1.83 (2)
O(3)-H(1)	0.99	P(3)-C(51)	1.85 (2)
Cl(1)-H(1)	2.13	P(3)-C(61)	1.84 (2)
C(1)-O(1)	1.21 (4)	P(4)-C(71)	1.84 (2)
C(2)-O(2)	1.10 (4)	P(4)-C(81)	1.85 (3)
	Nonbonded Distances		
Ir(1)-Ir(2)	3.148 (2)	O(2)-H(72)	2.75
P(1)-P(2)	3.06 (1)	O(2)-H(44)	2.79
P(3)-P(4)	3.08 (1)	O(3)-H(1C4)	2.67
Cl(1)-H(2C3)	2.58	C(1)-H(62)	2.67
O(1)-H(74)	2.61	C(1)-H(16)	2.69
O(1)-H(84)	2.87	C(2)-H(46)	2.55
O(3)-Cl(1)	3.10 (2)	C(2)-H(72)	2.72
O(2)-H(43)	2.71		

such, the overall geometry closely resembles that of other "A-frames"[35,36] and is especially close to that of the rhodium analogue $[Rh_2(CO)_2(\mu\text{-}OH{\cdot}Cl)(DPM)_2]$.[21b]

The relatively long Ir(1)–Ir(2) separation of 3.148 (2) Å (see Table VI) suggests that there is no formal metal–metal bond. This distance is significantly longer than those observed in similar compounds containing Ir–Ir single bonds (range 2.779 (1)–2.893 (2) Å)[13,23,37-40] and is also longer than the intraligand P–P distances (ca. 3.07 Å) in the compound, suggesting a lack of attraction between the metals. The absence of a formal metal–metal bond is also consistent with conventional electron-counting techniques which give each Ir atom a 16-electron configuration.

Certainly the most interesting aspect of the structure is the presence of the bridging OH·Cl moiety. This group can be most logically considered as a bridging hydroxide ligand having the chloride anion hydrogen bonded to it, although this is not the only interpretation, as will be mentioned later. The hydrogen atom of the hydroxy group did not refine well, even though it was clearly defined on difference Fourier maps. Its observed and unrefined position yields an approximately linear O(3)–H(1)–Cl angle of ca. 163° and short O(3)–H(1) and H(1)–Cl contacts of 0.99 and 2.13 Å, respectively, suggesting the presence of hydrogen bonding involving O(3), H(1), and Cl. Furthermore, the O(3)–Cl distance of 3.10 (2) Å is shorter than a normal van der Waals contact of between 3.20 and 3.40 Å again suggestive of hydrogen bonding. All parameters are in agreement with those found in other hydrogen-bonded systems.[41] The strength of this O–H–Cl interaction is further evidenced by the failure of the chloride ion to dissociate in solution (vide infra). It also can be seen that the chloride ion is interacting with one of the DPM methylene hydrogens resulting in a Cl–H(2C3) contact (ca. 2.58 Å) which is again less than the van der Waals distance. The OH·Cl moiety is symmetrically bonded to both metals, with Ir–O distances of 2.07 (2) and 2.06 (2) Å and an Ir(1)–O(3)–Ir(2) angle of 99.4 (8)°; these values compare rather well with those in the rhodium analogue.[21b] As Figure 2 shows, the hydrogen atom of the hydroxy group lies well above the Ir(1)–Ir(2)–O(3) plane (by ca. 0.67 Å), suggesting sp^3 hybridization of the oxygen atom.

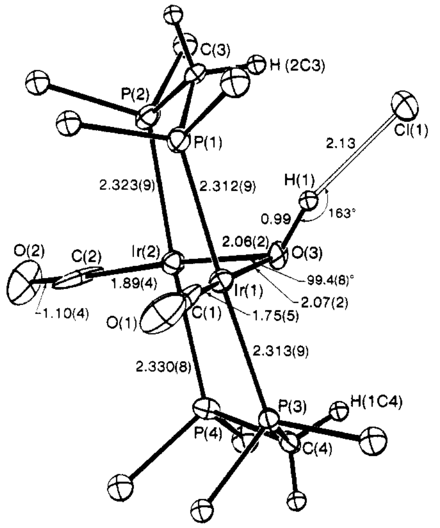

Figure 2. The inner coordination sphere of the title complex along with some relevant bond lengths and angles.

Within the DPM framework the parameters are unexceptional (see Tables VI and VII) and are similar to those found in related structures. Both DPM methylene groups are folded toward the bridging OH·Cl group allowing the phenyl rings to occupy the relatively open positions on the opposite side of the complex. This orientation also allows the above-mentioned interaction between the methylene protons and the chloride ion to occur. As is also shown in Figure 2, the $Ir_2(DPM)_2$ framework is skewed somewhat, with P–Ir–Ir–P torsion angles of ca. 6.5° (see Table VII). However, this slight degree of skewing is not unusual. The carbonyl groups are also quite normal and are essentially trans to the Ir–O bonds leading to a rather undistorted "A-frame" geometry.

(b) Preparation and Characterization of Compounds. The studies of Yoshida and co-workers on catalysis of the WGS reaction by mononuclear rhodium phosphine complexes demonstrated the involvement of metal hydroxides in the catalytic cycle, part of which is outlined in eq 2–5.[14] In this system, it was proposed that

$$[Rh(OH)(CO)(PR_3)_2] \underset{S\,=\,\text{solvent}}{\overset{S}{\rightleftharpoons}} [Rh(CO)(S)(PR_3)_2][OH] \quad (2)$$

$$[Rh(CO)(S)(PR_3)_2][OH] \xrightarrow[-S]{CO} [Rh(CO)_2(PR_3)_2][OH] \quad (3)$$

$$[Rh(CO)_2(PR_3)_2][OH] \rightarrow [Rh(CO)(CO_2H)(PR_3)_2] \quad (4)$$

$$[Rh(CO)(CO_2H)(PR_3)_2] \xrightarrow[-CO_2]{} [RhH(CO)(PR_3)_2] \quad (5)$$

hydroxide ion first dissociates from the complex and subsequently attacks an electrophilic CO ligand. We were interested in developing complexes related to $[Rh(OH)(CO)(PR_3)_2]$, in which as many ligands as possible could be actively involved in the reaction of interest (in this case the WGS reaction), and therefore set out to synthesize a binuclear iridium analogue of the above hydroxide, namely, *trans*-$[Ir(OH)(CO)(DPM)]_2$. We had previously observed

---

(35) Cowie, M.; Dwight, S. K. *Inorg. Chem.* **1979**, *18*, 2700.

(36) Kubiak, C. P.; Eisenberg, R. *Inorg. Chem.* **1980**, *19*, 2726.

(37) Sutherland, B. R.; Cowie, M. *Organometallics* **1984**, *3*, 1869. The compound $[Ir_2Cl_2(CO)_2(\mu\text{-}CH_3O_2CC_2CO_2CH_3)(DPM)_2]$ has an Ir–Ir bond of 2.7793 (3) Å.

(38) Sutherland, B. R.; Cowie, M., unpublished results on the structure of the Ir–Ir bonded compound $[Ir_2Cl_4(CO)_2(DPM)_2]$ show that it has an Ir–Ir distance of 2.789 Å.

(39) Mague, J. T.; Klein, C. L.; Majeste, R. J.; Stevens, E. D. *Organometallics* **1984**, *3*, 1860.

(40) Kubiak, C. P.; Woodcock, C.; Eisenberg, R. *Inorg. Chem.* **1980**, *19*, 2733.

(41) Vinogradov, S. N.; Linnell, R. H. "Hydrogen Bonding"; Van Nostrand-Reinhold: New York, 1971.

Table VII. Selected Angles (deg) in $[Ir_2(CO)_2(\mu\text{-}OH\bullet Cl)(DPM)_2]$

(a) Bond Angles					
O(3)–Ir(1)–C(1)	174.0 (14)	Ir(1)–P(1)–C(3)	112.8 (10)	C(4)–P(4)–C(71)	105.3 (12)
O(3)–Ir(1)–P(1)	92.8 (6)	Ir(1)–P(2)–C(3)	113.5 (10)	C(4)–P(4)–C(81)	104.6 (13)
O(3)–Ir(1)–P(3)	84.1 (6)	Ir(1)–P(3)–C(4)	112.3 (11)	C(71)–P(4)–C(81)	101.6 (12)
C(1)–Ir(1)–P(1)	87.9 (12)	Ir(2)–P(4)–C(4)	112.2 (10)	P(1)–C(3)–P(2)	115 (2)
C(1)–Ir(1)–P(3)	95.0 (12)	Ir(1)–P(1)–C(11)	116.2 (7)	P(3)–C(4)–P(4)	116 (2)
P(1)–Ir(1)–P(3)	176.8 (3)	Ir(1)–P(1)–C(21)	113.9 (8)	P(1)–C(11)–C(12)	118.2 (9)
O(3)–Ir(2)–C(2)	175.9 (12)	Ir(2)–P(2)–C(31)	117.6 (7)	P(1)–C(11)–C(16)	121.8 (9)
O(3)–Ir(2)–P(2)	90.7 (6)	Ir(2)–P(2)–C(41)	117.1 (7)	P(1)–C(21)–C(22)	119.2 (10)
O(3)–Ir(2)–P(4)	85.5 (6)	Ir(1)–P(3)–C(51)	112.9 (7)	P(1)–C(21)–C(26)	120.7 (10)
C(2)–Ir(2)–P(2)	93.3 (10)	Ir(1)–P(3)–C(61)	118.3 (7)	P(2)–C(31)–C(32)	116.3 (10)
C(2)–Ir(2)–P(4)	90.5 (10)	Ir(4)–P(4)–C(71)	114.6 (7)	P(2)–C(31)–C(36)	123.7 (9)
P(2)–Ir(2)–P(4)	176.2 (4)	Ir(2)–P(4)–C(81)	117.3 (8)	P(2)–C(41)–C(42)	119.7 (9)
Ir(2)–O(3)–Ir(2)	99.4 (8)	C(3)–P(1)–C(11)	105.6 (12)	P(2)–C(41)–C(46)	120.3 (9)
Ir(1)–O(3)–H(1)	119	C(3)–P(1)–C(21)	105.1 (13)	P(3)–C(51)–C(52)	121.9 (10)
Ir(2)–O(3)–H(1)	111	C(31)–P(2)–C(41)	100.2 (10)	P(3)–C(51)–C(56)	118.0 (11)
Ir(1)–C(1)–O(1)	176 (4)	C(3)–P(2)–C(31)	102.0 (12)	P(3)–C(61)–C(62)	119.9 (9)
Ir(2)–C(2)–O(2)	176 (4)	C(3)–P(2)–C(41)	104.2 (12)	P(3)–C(61)–C(66)	120.1 (9)
O(3)–H(1)–Cl(1)	163	C(11)–P(1)–C(21)	102.2 (10)	P(4)–C(71)–C(72)	117.5 (9)
		C(4)–P(3)–C(51)	103.0 (13)	P(4)–C(71)–C(76)	122.6 (10)
		C(4)–P(3)–C(61)	104.0 (13)	P(4)–C(81)–C(82)	118.0 (12)
		C(51)–P(1)–C(21)	104.8 (10)	P(4)–C(81)–C(86)	122.1 (12)
(b) Torsion Angles					
P(1)–Ir(1)–Ir(2)–P(2)	6.6 (3)	P(1)–Ir(1)–Ir(2)–P(4)	176.0 (3)		
P(3)–Ir(1)–Ir(2)–P(4)	6.7 (3)	P(3)–Ir(1)–Ir(2)–P(2)	170.7 (3)		

the following equilibrium in solution,[23] involving the closely related chloro species, and reasoned that the hydroxide

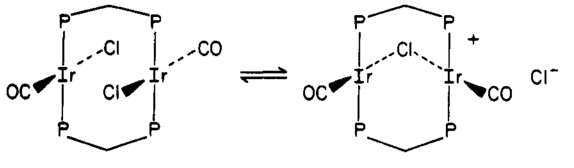

I II

complex might behave similarly. Such reversible hydroxide ion dissociation would parallel that shown in eq 2 for the mononuclear system suggesting the potential for catalysis of the WGS reaction by these binuclear complexes. However, the reaction between *trans*-$[IrCl(CO)(DPM)]_2$ and excess NaOH does not yield a dihydroxy analogue of species I as was anticipated. Instead, compound 1, which analyzes as $[Ir_2Cl(OH)(CO)_2(DPM)_2]$, is obtained. This species, shown by its $^{31}P\{^1H\}$ NMR spectrum to be symmetrical on the NMR time scale, has two rather low carbonyl stretches at 1904 and 1882 cm^{-1} and is a nonelectrolyte in CH_2Cl_2. Although no stretch attributable to an O–H moiety was obvious in the IR spectrum, careful examination of the ^1H NMR spectrum showed a broad quintet at δ 4.85 due to the hydroxide hydrogen atom coupled to four phosphorus nuclei. As discussed earlier, the X-ray structure determination clearly established the structure shown below for this compound, in which the

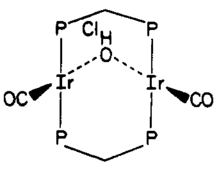

1

bridging hydroxide group is hydrogen bonded to the chloride ion. It seems, based on the lack of conductivity and on the similarities in the solution and solid IR spectra, that the chloride ion remains hydrogen bound in CH_2Cl_2 solution. The hydrogen bonding involving the hydroxide group accounts for our failure to observe the O–H stretch in the region normally associated with a free O–H moiety. In the ^1H NMR spectrum of 1 the resonances for the DPM methylene protons are rather broad and unresolved with one being shifted downfield from what is usually observed, suggesting that the interaction between the chloride ion and the methylene group, which was observed in the X-ray structure, persists in solution. Since there are only two methylene resonances in the ^1H NMR spectrum and since the $^{31}P\{^1H\}$ resonance appears as a singlet down to –40 °C, a rapid fluxional process must be occurring which transfers the chloride ion from one methylene group to the other either by an inter- or intramolecular process.

Although complex 1 can be viewed as containing a bridging hydroxide group with a hydrogen-bound chloride ion, an alternate, if somewhat less attractive, viewpoint is to consider it as a bridging oxide complex with a hydrogen-bound HCl molecule. This latter view is not totally unreasonable since a comparison of the carbonyl stretches in 1 with those in the analogous sulfide-bridged complex $[Ir_2(CO)_2(\mu\text{-}S)(DPM)_2]$[40] (1918, 1902 cm^{-1}) indicates that they are very similar.

Treatment of compound 1 with one equivalent of $HBF_4 \cdot Et_2O$ results in the formation of $[Ir_2(CO)_2(\mu\text{-}OH)(DPM)_2][BF_4]$ (2), presumably through loss of HCl (although no attempt was made to detect this). The O–H stretch for the bridging hydroxide group in 2 appears as a weak band at 3498 cm^{-1}, and the ^1H NMR resonance appears as a quintet at δ 2.03 ppm with $^3J_{P-H}$ = 3.1 Hz. The carbonyl bands in the IR spectrum, although still quite low (1959, 1943 cm^{-1}), are higher than in the parent compound 1, reflecting the positive charge of compound 2. All of the spectroscopic parameters (see Tables I and II) are consistent with compound 2 having an "A-frame" geometry like compound 1, but without the chloride ion. Another route for the preparation of 2 from 1 by reaction with Ag^+ does yield 2 in ca. 70% yield; unfortunately other products are also produced which appear to contain coordinated Ag^+, as suggested by the observation of long-range Ag–P coupling in the $^{31}P\{^1H\}$ NMR spectra. Owing to the difficulties in separating these Ag-containing impurities from 2, the reaction of 1 with acid is the route of choice. Silver adducts of these binuclear iridium complexes have been obtained by another route and will be the subject of a subsequent publication.[42]

---

[42] Cowie, M.; Sutherland, B. R., unpublished results.

The reactions of compounds **1** and **2** with CO take two rather different routes. When a CH_2Cl_2 solution of **1** is treated with an atmosphere of CO (under ambient conditions), a new compound **3** can be isolated in 90% yield as bright yellow crystals. In the solid state **3** displays five carbonyl stretches in the IR spectrum but shows only four bands in solution (see Table I). Although elemental analyses of these crystals shows the presence of two chlorine atoms per dimer, ^1H NMR spectra clearly show that these chlorines are due to CH_2Cl_2 of solvation and, furthermore, recrystallization of **3** from THF/ether yields **3** with no CH_2Cl_2 appearing in the ^1H NMR and with no chlorine detected in the elemental analyses. Apart from the resonances due to the DPM phenyl and methylene protons no other resonances appear between 15 and −40 ppm in the ^1H NMR spectrum. The NMR data for **3** indicate that it is fluxional in solution. At 20 °C the $^{31}P\{^1H\}$ NMR spectrum shows a sharp singlet characteristic of a symmetrical species, but at −80 °C the spectrum shows two broad unresolved multiplets at δ −18.6 and −24.2. Similarly, at 20 °C only one carbonyl resonance is observed (δ 183) in the ^{13}C NMR spectrum compared with two equally weighted resonances (δ 175 and 188) at −80 °C. On the basis of the information and the loss of CO from **3** to give **4** (vide infra), compound **3** is formulated as $[Ir_2(CO)_4(DPM)_2]$. The possibility that **3** is a pentacarbonyl is ruled out by electron counting, since in order to avoid exceeding an 18-electron configuration at each metal one carbonyl group would have to be bridging without an accompanying Ir–Ir bond and no carbonyl stretch low enough for this situation[19,43–45] is observed. In addition, the two equally weighted carbonyl resonances in the ^{13}C NMR spectrum suggest a four-carbonyl species. Compound **3** is very susceptible to CO loss, such that flushing the solution with N_2 causes it to darken, yielding a new compound $[Ir_2(CO)_3(DPM)_2]$, **4**, which in the solid has three carbonyl bands in the IR spectrum at 1950, 1936, and 1857 cm^{-1}. Although the rhodium analogue has been assigned[13] the "A-frame" structure shown in III, we reject this for both the Ir and Rh compounds since the stretch for the bridging carbonyl ligand in the absence of a metal–metal bond should be much lower as has been observed in all structurally characterized complexes of this type.[19,43–45] In fact, on the basis of the spectral parameters, we propose that compound **4** has a static structure like IV, but which is fluxional in solution. At room temperature, the time-averaged structure of **4** must be symmetrical since the $^{31}P\{^1H\}$ NMR spectrum appears as a sharp singlet and the ^1H NMR of the DPM methylene region appears as a single sharp quintet at this temperature. As the temperature is lowered to −80 °C, the $^{31}P\{^1H\}$ resonance broadens to an unresolved multiplet at δ −3.5 and the ^1H resonance for the CH_2 protons broadens also. Although the infrared band at 1857 cm^{-1} is suggestive of a bridging carbonyl group, no resonance shows up at low enough field in the ^{13}C NMR spectrum to correspond to such a group; at 20 °C there are two sharp resonances at δ 183 and 187 (corresponding to two and one carbonyls, respectively) while at −80 °C the three equally weighted resonances are also characteristic of terminal carbonyls, at δ 175, 185, and 188. We suggest therefore that the low carbonyl stretch does not correspond to a bridging CO but corresponds to that terminal CO which is bound to the 16-electron center; there are no other π-accepting groups competing for electron density on this low oxidation state metal so the low CO stretch is not surprising, particularly when it is recalled that in the Ir(I) complex **1**, the CO stretches were not much higher. The structure of the tetracarbonyl species **3** is presumably closely related to **4**, with each metal having a five-coordinate, 18-electron configuration and two carbonyl ligands as shown above. Although we have not attempted to analyze the fluxionalities of **3** and **4** in detail, it should be noted that the five-coordinate metal centers should be prone to fluxionality.

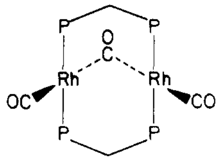

III

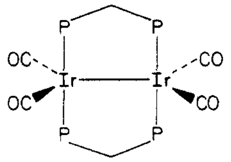

3

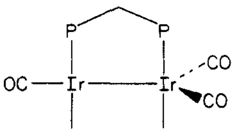

IV

The formation of the Ir(0) complexes **3** and **4** from **1** is novel; in particular it should be noted that this does not occur with the analogous Rh species.[21b] At the present time, it is not clear how this transformation takes place and attempts to observe intermediates in the $^{31}P\{^1H\}$ NMR spectra of the reaction mixture at −80 °C using stoichiometric amounts of CO were unsuccessful; only compounds **1** and **4** were observed.

The corresponding reaction of compound **2** with excess CO also proceeds readily at room temperature resulting in the eventual production of a red-purple solid, **5**. This species displays three carbonyl bands in the IR spectrum at 1979, 1967, and 1826 cm^{-1} and shows a quintet in the ^1H NMR spectrum at −9.44 ($^2J_{PH}$ = 9.4 Hz). On the basis of this information and the observation of a singlet in the $^{31}P\{^1H\}$ NMR spectrum, **5** can be formulated as $[Ir_2(CO)_2(\mu\text{-}H)(\mu\text{-}CO)(DPM)_2]^+$ as shown, similar to that reported for the Rh analogue.[13] Compound **5** can actually be isolated in two different forms in the solid state: the aforementioned red-purple solid, **5a**, and a dark orange form, **5b**. These two solids differ only in the positions of the bridging carbonyl and the BF_4^- stretches in the IR (see Table I). This is most likely due to crystal packing forces, since in solution both have identical spectroscopic properties which more closely resemble those of the orange isomer. There appears to be no systematic method for obtaining one or the other form, and **5** is often isolated as a mixture of the two. An X-ray study has been carried out on the dark orange form and confirms the structure as shown above.[46]

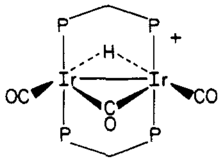

5

---

(43) Colton, R.; McCormick, M. J.; Pannan, C. D. *Aust. J. Chem.* **1978**, *31*, 1425.

(44) Brown, M. R.; Keith, A. N.; Manojlović-Muir, Lj.; Muir, K. W.; Puddephatt, R. J.; Seddon, K. R. *Inorg. Chim. Acta* **1979**, *34*, L223.

(45) Mague, J. T.; DeVries, S. H. *Inorg. Chem.* **1982**, *21*, 1632.

(46) Cowie, M.; Sutherland, B. R., manuscript in preparation. The structure has converged at R = 0.031 and R_w = 0.043, and the bridging hydride ligand has been located and refined.

In the slow stepwise addition of CO to compound **2** at −40 °C a minor species is observed at intermediate times, together with compounds **2** and **5**. This intermediate is observed as a singlet at δ 15.6 in the $^{31}P\{^1H\}$ NMR spectrum, and its appearance is accompanied by the growth of two new IR bands at 3687 and 1604 cm^{-1}. It may be that this intermediate is a metallocarboxylic acid complex since the IR bands agree well with those previously reported for such species.[47-50] No other features in the carbonyl region of the IR spectra prove to be helpful in assigning a structure to this intermediate since these spectra are dominated by bands due to compounds **2** and **5**. We were also unable to observe the M–C(O)OH proton in the ^1H NMR spectrum. CO_2 loss from this metallocarboxylic intermediate could occur by β-hydride transfer to the metals yielding compound **5**. Although this spectroscopic evidence above is not consistent with a formate intermediate, one cannot be ruled out since the reaction of $[Ir_2(CO)_2(CH_3CN)_2(\mu\text{-}CO)(DPM)_2][BF_4]$ with sodium formate yields compound **5** as the only observed product (see Experimental Section). When the transformation of **2** to **5** is carried out in deuterated solvents, no evidence of deuterium incorporation into **5** is observed indicating that the hydrido ligand in **5** does originate from the hydroxy group in **2**.

Compound **5** can also be formed by the protonation of **4** with 1 equiv of $HBF_4\cdot Et_2O$; however, the reverse deprotonation has not been effected; even the strong base 1,8-bis(dimethylamino)naphthalene[51] leaves **5** unchanged.

The analogous rhodium hydride complex $[Rh_2(CO)_2(\mu\text{-}H)(\mu\text{-}CO)(DPM)_2]^+$ was found to be a catalyst in the WGS reaction, under relatively mild conditions,[13] however, none of the intermediates in the reaction was clearly characterized. With the iridium analogue we seemed to have an opportunity to examine in detail a model system for this reaction and thereby learn more about the possible steps involved. The reaction of $[Ir_2(CO)_2(\mu\text{-}OH)(DPM)_2]^+$ with CO accomplishes one of these steps, namely, the oxidation of CO to CO_2. The other important step, the generation of H_2, was accomplished in the Rh system through the reaction of $[Rh_2(CO)_2(\mu\text{-}H)(\mu\text{-}CO)(DPM)_2]^+$ with strong acid giving an uncharacterized dicationic rhodium complex.[13] We find that compound **5** also reacts with the strong acid $HBF_4\cdot Et_2O$ but in this case H_2 is not produced, and we instead isolate the dihydride $[Ir_2H(CO)_2(\mu\text{-}H)(\mu\text{-}CO)(DPM)_2][BF_4]_2$. The IR spectrum of **6** (see Table I) shows an Ir–H stretch at 2108 cm^{-1} and carbonyl bands at 2046, 1961, and 1833 cm^{-1}. The $^{31}P\{^1H\}$ NMR spectrum (see Table II) indicates that the species is unsymmetrical, and the ^1H NMR spectrum shows two high-field resonances, integrating as one hydrogen each. The high-field resonance at δ −13.2 appears as a sharp triplet of doublets ($^2J_{P-H}$ = 10.5 Hz, $^2J_{H-H}$ = 1.6 Hz) corresponding to a terminal hydride coupled to two adjacent phosphorus nuclei and to another hydrogen, and the downfield resonance at −7.1 ppm appears as a broad unresolved peak. It is probable that the latter resonance is due to the bridging hydride which is coupled to two pairs of chemically inequivalent P nuclei and to the terminal hydride. Our failure to resolve this resonance into its expected triplet of triplets of doublets is not surprising given the probable magnitudes of the coupling constants (see Table II). Two structures are possible for this diprotonated species as shown. We suggest that compound **6** has structure VI, owing to its failure to reductively eliminate H_2 (vide infra). Although the H–H coupling observed is rather small for what might be expected for trans hydride ligands and is more in line with what is usually observed for cis hydrides,[52] we have observed similarly small coupling constants for $[Ir_2H(CO)_2(\mu\text{-}H)_2(DPM)_2]^+$, in which the terminal hydride is trans to one of the bridging ones.[53] We also suggest, based on the facile loss of H_2, that protonation of the rhodium analogue[13] yields a structure analogous to V. A subsequent paper dealing with the structure of **5** will attempt to rationalize this difference between the Rh and Ir analogues.[46]

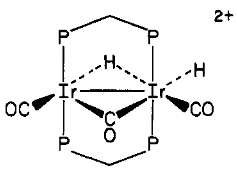

V

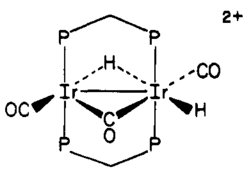

VI

Upon standing in solution for about 1 week **6** rearranges to a new compound, **7**, in which the two hydride and three carbonyl ligands are now all terminal; the ^1H NMR spectrum shows two high field triplets indicating coupling of each hydride to a pair of phosphorus nuclei and the carbonyl stretches correspond to terminal groups. the $^{31}P\{^1H\}$ NMR spectrum indicates that the molecule is still unsymmetrical, making structures VII–IX the most probable. Of these we favor VII since **7** can also be obtained by the rapid reaction of $[Ir_2(CO)_2(MeCN)_2(\mu\text{-}CO)(DPM)_2]^{2+}$ (**10**) with H_2, consistent with the oxidative addition of H_2 occurring in a concerted manner leading to a cis hydride complex. Significantly no evidence of **6** is observed in the reaction of **10** with H_2, further suggesting a trans arrangement of hydrides for **6**.

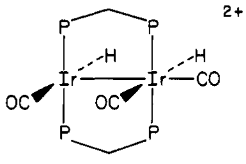

VII

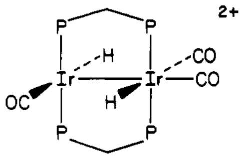

VIII

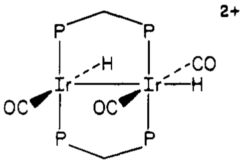

IX

Although the conductivity measurements for compounds **6** and **7** (and also of **8**) are too low in CH_2Cl_2 for normal 2:1 electrolytes, they are normal in nitromethane. Furthermore, their spectral and chemical information leaves no doubt concerning their stoichiometries. For example, compound **10**, shown to be a normal 2:1 electrolyte, reacts with H_2 to yield **7**, and as will be explained, **10** can ulti-

---

[47] Sweet, J. R.; Graham, W. A. G. *Organometallics* **1982**, *1*, 982.

[48] Catellani, M.; Halpern, J. *Inorg. Chem.* **1980**, *19*, 982.

[49] Grice, N.; Kao, S. C.; Pettit, R. *J. Am. Chem. Soc.* **1979**, *101*, 1627.

[50] Deeming, A. J.; Shaw, B. L. *J. Chem. Soc. A* **1969**, 443.

[51] [1,8-Bis(dimethylamino)naphthalene] = Proton Sponge.

[52] Typical coupling on Ir–phosphine hydrides between cis hydrides fall in the range 2–5 Hz, but in all cases the hydrides are on the same metal. See: Guilmet, E.; Maisonnat, A.; Poilblanc, R. *Organometallics* **1983**, *2*, 1123. In an analogous binuclear Pt complex in which a bridging hydrido ligand is trans to a terminal hydride, the H–H coupling constant is 15 Hz. See: Puddephatt, R. J.; Azam, K. A.; Hill, R. H.; Brown, M. P.; Nelson, C. D.; Moulding, R. P.; Seddon, K. R.; Grossel, M. C. *J. Am. Chem. Soc.* **1983**, *105*, 5642.

[53] Cowie, M.; Sutherland, B. R., submitted for publication in *Organometallics*.

mately be regenerated from **7**. We conclude that the low conductivity measurements in CH_2Cl_2 are due to ion pairing in this solvent of a low dielectric constant. In solvents such as acetone, deprotonation of these dihydrides to give **5** occurred.

Attempts to induce H_2 loss from either **6** or **7** by refluxing in CH_2Cl_2 for up to 4 h failed, and only starting materials were recovered. However, H_2 loss can be induced by two routes, first by the addition of CO and second by refluxing in acetonitrile. When either **6** or **7** is stirred under an atmosphere of CO, an immediate reaction occurs and a white solid (**8**) can be isolated. The IR spectrum of **8** shows carbonyl bands at 2080, 2061, 2038, and 2017 cm^{-1}, and the ^1H NMR spectrum shows a high-field quintet ($^2J_{P-H}$ = 5.1 Hz), integrating as two protons, for the two bridging hydrogens. On the basis of these data and the $^{31}P\{^1H\}$ NMR spectrum which shows a singlet, we propose the following structure for **8**. Heating this species in CH_2Cl_2 regenerates only **6**, again suggesting the trans hydride geometry VI for this latter species; loss of a terminal carbonyl group in **8** would readily yield **6** by moving one H to a terminal site and one terminal carbonyl to the vacated bridging position.

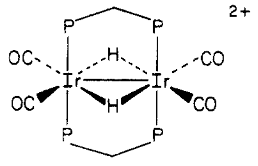

8

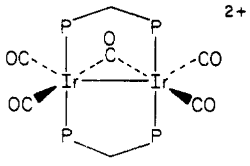

9

Although the major product from the reaction of **6** with CO is still a hydride, another product is observed in about 10% yield. This was subsequently identified as $[Ir_2(CO)_4(\mu\text{-}CO)(DPM)_2][BF_4]_2$, **9**, which was prepared independently from the reaction of $[Ir_2Cl(CO)_3(\mu\text{-}CO)(DPM)_2][Cl]$ with 2 equiv of $AgBF_4$ under a CO atmosphere (see Experimental Section). The infrared spectrum of **9** in the solid shows four terminal and one bridging carbonyl bands indicating that compound **9** probably has the structure shown above in which the geometry is similar to that observed for $[Ir_2Cl_2(CO)_2(\mu\text{-}CO)(DPM)_2]$.[23]

The production of some **9** from the reaction of **6** and **7** with CO shows that reductive elimination of H_2 has occurred, presumably proceeding through an intermediate having the hydride ligands mutually cis. Compound **8** also converts to **9**, albeit very slowly, when left under an atmosphere of CO for up to 2 weeks. H_2 removal from **7** can also be partially effected by heating in acetonitrile for ca. 20 or more min, yielding the tricarbonyl species $[Ir_2(CO)_2(CH_3CN)_2(\mu\text{-}CO)(DPM)_2]^{2+}$ (**10**). This latter product can also be prepared in high yield by the reaction of **9** with acetonitrile (see Experimental Section) and has carbonyl bands in the IR spectrum at 2005, 1980, and 1731 cm^{-1} and bands due to the acetonitrile ligands at 2312 and 2284 cm^{-1}. On the basis of these data and the $^{31}P\{^1H\}$ NMR spectrum which indicate that **10** is symmetric, the two structures X and XI are possible. Although differentiation of these two species based on the available data is not possible, the low stretch for the bridging carbonyl group may suggest that it is trans to the better σ-donor acetonitriles rather than the π-accepting carbonyls. Although this hydride-free product is obtained readily in refluxing acetonitrile, it is obtained as only a minor product (ca. 10% yield); the other products have not been identified and their number increases with increased reflux time.

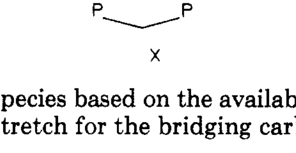

X

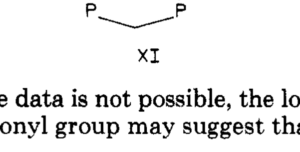

XI

Both compounds **9** and **10** react with hydroxide ion. The reaction of **9** with 1 equiv of $NMe_4OH{\cdot}5H_2O$ results in the formation of only compound **5**. This reaction may occur by OH^- attack at one of the carbonyl ligands resulting in the formation of a metallocarboxylic acid species. The high carbonyl stretches for the terminal carbonyls in the dicationic species **9** suggest that these groups will be susceptible to nucleophilic attack. Direct attack at the metals is less likely since both metals have 18-electron configurations and CO dissociation would first have to occur. Subsequent loss of CO_2 from the metallocarboxylic intermediate would then yield a tetracarbonyl hydride complex which after CO loss would yield **5** (vide infra).

Reaction of **10** with OH^- also occurs readily but, based on the products obtained, appears to proceed by a different route. In this reaction, both compounds **2** and **5** are obtained, in the ratio of 3:1, respectively. Furthermore, if the reaction vessel is flushed with N_2 during the course of the reaction, this ratio changes to 5:1. This information suggests that in this case OH^- attack does not occur directly at a carbonyl group since this would be expected to yield, after CO_2 loss, the hydride $[Ir_2(CO)_2(\mu\text{-}H)(DPM)_2]^+$, which is not observed. The observation of the hydroxy-bridged species **2** indicates that OH^- attack occurs at the metals at some stage of the reaction. We propose that the reaction of **10** with OH^- occurs with coordination of the hydroxide ligand at the metals, accompanied by acetonitrile loss to give $[Ir_2(CO)_2(\mu\text{-}OH)(\mu\text{-}CO)(DPM)_2]^+$ (**11**), a short-lived intermediate which is not observed. This proposed intermediate is very similar to the well-characterized chloro-bridged species $[Ir_2(CO)_2(\mu\text{-}Cl)(\mu\text{-}CO)(DPM)_2]^+$,[23] and CO loss from this species would yield one of the observed products, **2**. We expect that CO loss from **11** would be quite facile since as described previously, when the stepwise addition of CO to **2** is monitored, such a tricarbonyl intermediate is never observed. The other product in the reaction of **10** with hydroxide ion, **5**, could arise by several routes, although it is clear that on the basis of its reduced yield when the solution is flushed with N_2, additional CO is required for its formation. One possibility is that CO lost from **11** can be picked up by compound **10** to give either **9** or a dicationic tetracarbonyl species and that subsequent nucleophilic attack by OH^- at one of the carbonyl groups yields **5** after CO_2 loss. However, **11** may itself be an intermediate in the production of **5**; it could coordinate additional CO lost by other molecules of **11** and after intramolecular hydroxide migration to a carbonyl group could yield a metallocarboxylic acid intermediate, which through loss of CO_2 would yield **5**. Although such an intramolecular pathway has not often been proposed,[54] we feel that it cannot be ruled out as a viable pathway.

Consistent with the attack of the OH^- at the metal is the observation that the reaction of **10** with methoxide ion does not yield a methoxycarbonyl species but instead gives **5** in essentially quantitative yield. Again, it seems that methoxide attack at the metals occurs to yield an intermediate, $[Ir_2(CO)_2(OMe)(\mu\text{-}CO)(DPM)_2]^+$, which then β-hydride eliminates to give **5**.

(c) A Model Cycle for Water-Gas Shift Catalysis. We have attempted to demonstrate in the foregoing

---

[54] Appleton, T. G.; Bennett, M. A. *J. Organomet. Chem.* **1973**, *55*, C88.

Scheme I

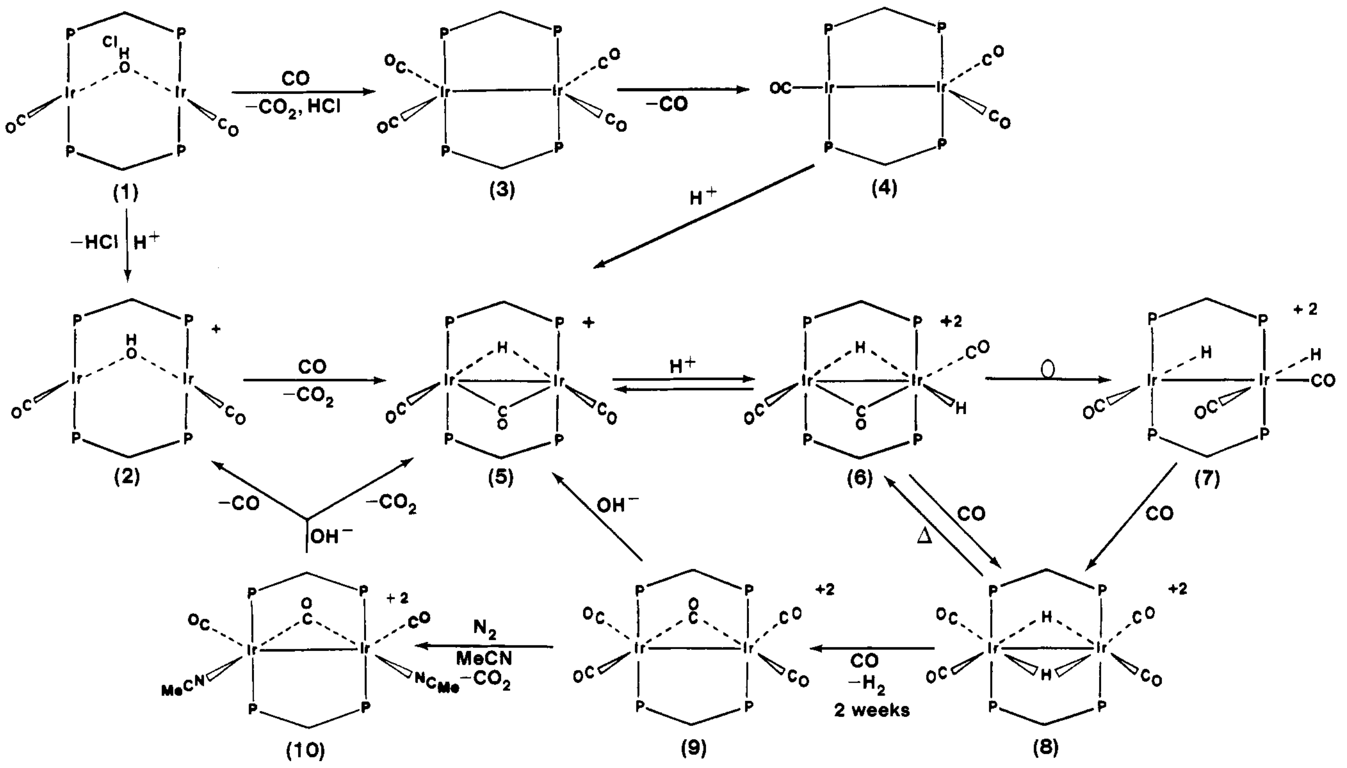

chemistry that hydroxy-bridged species such as **2** could be involved as catalysts in the WGS reaction. These reactions are summarized in Scheme I, depicting the conversion of CO and H_2O (OH^- + H^+) to CO_2 and H_2. In this scheme, we show the facile conversion of the hydroxy-bridged species **2** into the hydrido-bridged complex **5** and CO_2, and subsequent protonation of this hydride to give a dihydride species, **6**, which under CO ultimately loses H_2 to give the dicationic pentacarbonyl complex **9**. At this stage either reaction with hydroxide ion regenerates the hydrido-bridged species or, if reaction with the dicationic tricarbonyl complex **10** occurs, both the hydroxide- and hydride-bridged complexes are obtained. In any event, the WGS cycle is complete with the obvious slow step being H_2 loss. In our system the model catalyst precursor is $[Ir_2(CO)_2(\mu\text{-}OH)(DPM)_2]^+$; however, the involvement of the hydride-bridged species $[Ir_2(CO)_2(\mu\text{-}H)(\mu\text{-}CO)(DPM)_2]^+$ in this cycle suggested to us that our chemistry may be applicable to the catalytic cycle reported by Eisenberg and co-workers which utilized the analogous rhodium hydride $[Rh_2(CO)_2(\mu\text{-}H)(\mu\text{-}CO)(DPM)_2]^+$ as the catalyst precursor[13] and therefore suggested that metal hydroxides might be involved in Eisenberg's cycle also. Although we have not carried out detailed kinetic studies on this system, parallel comparative runs using $[Rh_2(CO)_2(\mu\text{-}OH)(DPM)_2]^+$ and $[Rh_2(CO)_2(\mu\text{-}H)(\mu\text{-}CO)(DPM)_2]^+$ as catalyst precursors, under the conditions studied by Eisenberg and co-workers[13] (see Experimental Section), show that the two have equivalent turnover rates after a 48-h period (turnover rate $\simeq$ 0.15 equiv of CO_2/h). Furthermore, IR and NMR spectra run on the solid isolated from the catalytic reaction involving the hydroxy-bridged species indicates that the major species present is the hydrido-bridged tricarbonyl cation, showing that under the WGS conditions, the hydroxy-bridged species is converted into the hydrido-bridged catalyst precursor. However, it seems that *in this case*, hydroxide-containing rhodium complexes are not important as intermediates in the catalytic reaction. In particular, it had been noted that the addition of salts such as NaCl to solutions of $[Rh_2(CO)_2(\mu\text{-}H)(\mu\text{-}CO)(DPM)_2]^+$ enhanced the catalysis,[13] yet the addition of chloride salts to solutions of the hydroxide-bridged species results in the formation of $[Rh_2(CO)_2(\mu\text{-}OH\cdot Cl)(DPM)_2]$, which we have found is catalytically inactive under the same conditions, effectively ruling out such species as catalytic intermediates in the Eisenberg scheme. Nevertheless, the remainder of the scheme still has obvious relevance to WGS catalysis by $[Rh_2(CO)_2(\mu\text{-}H)(\mu\text{-}CO)(DPM)_2]^+$. Although no intermediates were characterized in the rhodium chemistry, our study on the analogous iridium chemistry clearly establishes the natures of three dihydride complexes and two dicationic species that are formed after H_2 loss (the penta- and tricarbonyl complexes). Such information, when extended to the analogous rhodium system, is valuable in formulating a reasonable scheme for the catalytic cycle. Although we do not suggest that the iridium cycle described exactly models the rhodium one, it seems reasonable that some of the key intermediates in the catalytic cycle resemble those characterized for iridium. We known for example that the hydride-bridged species analogous to **5** is involved, and we suggest that protonation of this species gives the rhodium analogue of **6** (except as in structure V) which reductively eliminates H_2 to give either the solvated analogue of **10** or, under CO, a higher carbonyl such as **9**. Reaction of these dicationic complexes with hydroxide ion could then regenerate the starting hydride by extrusion of CO_2 and either gain or loss of CO. The intermediates in the cycle about which we have little information are the metallocarboxylic acid complexes, and we are presently investigating these species in order to determine how the hydroxycarbonyl moieties interact with the two metal centers.

It is also important to note that although the complex $[Rh_2(CO)_2(\mu\text{-}OH)(DPM)_2]^+$ is not an important catalytic intermediate, such hydroxide-containing species may be important in WGS chemistry catalyzed by other rhodium or iridium complexes, and certainly the very facile conversion of the hydroxy-bridged complex **2** into the hydrido-bridged species **5** argues in favor of such a notion.

Acknowledgment. We thank the University of Alberta and the Natural Sciences and Engineering Research Council for support of this research, Johnson Matthey Ltd. for a generous loan of iridium trichloride, NSERC (Canada) for a graduate scholarship to B.R.S., Dr. R. G. Ball for collection of the X-ray data, Professor K. R. Grundy for communicating results prior to publication, and Mr. Jim A. Jenkins for technical assistance.

Note Added in Proof. The structure of $[Rh_2(CO)_3(DPM)_2]$, the Rh analogue of compound **4**, has recently been reported (Woodcock, C.; Eisenberg, R. *Inorg. Chem.* **1985**, *24*, 1285) and is shown to have an unusual structure, but one which is closely related to that proposed by us for compound **4**.

Supplementary Material Available: A listing of observed and calculated structure factor amplitudes and tables of anisotropic temperature factors and calculated hydrogen parameters (10 pages). Ordering information is given on any current masthead page.

Addition of Pseudohalogens to Vinyl- and Allylsilanes. Synthesis of 1-Substituted 2-(Alkylsilyl)- and 2-[(Alkylsilyl)methyl]aziridines Using Phase-Transfer Catalysis

Edmunds Lukevics,* Visvaldis V. Dirnens, Yuri S. Goldberg, Edvards E. Liepinsh, Maris P. Gavars, Ivars Ya. Kalvinsh, and Mariya V. Shymanska

Institute of Organic Synthesis, Latvian SSR Academy of Sciences, 226006, Riga, USSR

Received December 17, 1984

Addition of alkyl dichlorocarbamates to vinylsilanes by either an ionic or a radical mechanism occurs in an anti-Markownikoff orientation to give alkyl chloro[2-chloro-2-(trialkylsilyl)ethyl]carbamates (**3**). The reduction of **3** with aqueous sodium sulfite affords the corresponding alkyl [2-chloro-2-(trialkylsilyl)-ethyl]carbamates (**4**). *N*-[2-Chloro-2-(trialkylsilyl)ethyl]-*p*-toluenesulfonamides were obtained by the radical addition of *N*,*N*-dichloro-*p*-toluenesulfonamide (**5**) to trialkylvinylsilanes with subsequent reduction of the product. Addition of ethyl dichlorocarbamate to trimethylallylsilane (**9**) yields an equimolar mixture of β- and γ-adducts, while **5** reacts with **9** to give the Markownikoff adduct **7** regardless of the reaction mechanism. Intramolecular alkylation of carbamates **4a–c** and sulfonamide **7a** under solid–liquid phase-transfer conditions leads to 1-carbalkoxy- and 1-(*p*-tolylsulfonyl)-2-(trialkylsilyl)aziridines. 1-(Ethoxycarbonyl)- and 1-(*p*-tolylsulfonyl)-2-[(trimethylsilyl)methyl]aziridines were synthesized by similar cyclization. The possibility of intramolecular alkylation in a two-phase system under ultrasonic irradiation was demonstrated for carbamate **4c**.

Introduction

In our preliminary communication[1] we proposed a new method for the preparation of silicon-containing aziridines. The addition of methyl dichlorocarbamate to trimethylvinylsilane was found to give methyl chloro[2-chloro-2-(trimethylsilyl)ethyl]carbamate whose reduction with sodium hydrosulfite led to methyl [2-chloro-2-(trimethylsilyl)ethyl]carbamate. The latter was cyclized with sodium hydroxide powder using solid–liquid phase-transfer catalysis to afford 1-(methoxycarbonyl)-2-(trimethylsilyl)aziridine in good yield. Similarly, 1-(ethoxycarbonyl)-2-[(trimethylsilyl)methyl]aziridine was prepared from trimethylallylsilane and ethyl dichlorocarbamate. The present communication describes the general applicability of the above synthetic scheme for the preparation of N-substituted silicon-containing aziridines.

Results and Discussion

Addition of Pseudohalogens to Alkenylsilanes. Pseudohalogens, such as alkyl dichlorocarbamates and *N*,*N*-dichloroarenesulfonamides, are known to form adducts readily with alkenes.[2]

Scheme I

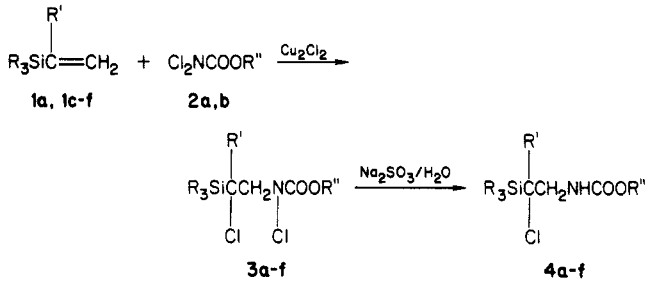

a, R = Me, R' = H, R" = Me, **b**, R = Me, R' = H, R" = Et, **c**, R = Et, R' = H, R" = Et, **d**, R = Me, R' = Br, R" = Et, **e**, R = Et, R' = Br, R" = Et, **f**, $R_3 = Et_2Me$, R' = COOMe, R" = Et

Thermal and photochemically induced addition of alkyl dichlorocarbamates follows a free radical mechanism.[2–6] *N*,*N*-Dichloro-*p*-toluenesulfonamide reacts with styrene[7,8] to yield an anti-Markownikoff adduct even when the re-

---

[1] Lukevics, E.; Dirnens, V. V.; Goldberg, Y. S.; Liepinsh, E. E.; Kalvinsh, I. Ya.; Shymanska, M. V. *J. Organomet. Chem.* **1984**, *268*, C29.

[2] Neale, R. S. *Synthesis* **1971**, 1.

[3] Foglia, T. A.; Swern, D. *J. Org. Chem.* **1965**, *30*, 3625.

[4] Foglia, T. A.; Swern, D. *J. Org. Chem.* **1968**, *33*, 766.

[5] Schrage, K. *Tetrahedron* **1969**, *29*, 3033, 3039.

[6] Neale, R. S.; Marcus, N. L.; Schepers, R. G. *J. Am. Chem. Soc.* **1966**, *88*, 3051.

[7] Seden, T. P.; Turner, R. W. *J. Chem. Soc.* **1968**, 876.

[8] Rybakova, N. A.; Petrovsky, P. V.; Okulevich, P. O.; Freidlina, R. Kh. *Izv. Akad. Nauk SSSR, Ser. Khim.* **1970**, 1574.

0276-7333/85/2304-1648$01.50/0 © 1985 American Chemical Society